

Analyzing-power measurements in the $^{48}\text{Ca}(p,n)^{48}\text{Sc}$ reaction at 134 MeV

B. D. Anderson, T. Chittrakarn, A. R. Baldwin, A. Fazely,* C. Lebo, R. Madey, and
J. W. Watson

Department of Physics, Kent State University, Kent, Ohio 44242

C. C. Foster

Indiana University Cyclotron Facility, Bloomington, Indiana 47405

(Received 15 February 1985)

Analyzing-power measurements were performed for the $^{48}\text{Ca}(p,n)^{48}\text{Sc}$ reaction at 134 MeV in about 6° steps from 0° to 60° . The overall neutron energy resolution varied from about 400 keV for angles out to 42° to about 700 keV at wider angles. Analyzing-power angular distributions were extracted for the $(\pi f_{7/2}, \nu f_{7/2}^{-1})$ octet of states, the 1^+ Gamow-Teller giant resonance, and the $T=4$, 1^+ state at $E_x=16.8$ MeV. All of these angular distributions are described reasonably well by "standard" distorted-wave impulse approximation calculations. A qualitative difference is observed in the analyzing power between the transitions to the low-lying 0^+ and 1^+ states compared to the transition to the high-lying 1^+ state. This difference appears to be associated with a sensitivity to the predominant particle-hole structure of the final states, viz., $(\pi f_{7/2}, \nu f_{7/2}^{-1})$ versus $(\pi f_{5/2}, \nu f_{7/2}^{-1})$. This sensitivity is ascribed to the difference in nonlocality contributions to the two different $1p1h$ excitations. Excitation-energy plots of the analyzing power were extracted at each angle. No characteristic signature of spin-transfer strength is observed in the region of the Gamow-Teller giant resonance.

I. INTRODUCTION

The $^{48}\text{Ca}(p,n)^{48}\text{Sc}$ reaction provides one of the best "test" cases for descriptions of the (p,n) reaction for several reasons. First, ^{48}Ca is believed to be a relatively good closed-shell nucleus, so that the reliability and accuracy of assumed structure calculations is improved over other possible nuclei. Secondly, ^{48}Ca has excess neutrons so that simple analog-state transitions are possible, including the transition to the analog of the ^{48}Ca ground state. Finally, in the simple shell model, the eight excess neutrons are in the $1f_{7/2}$ shell and can all participate in spin-transfer transitions to the $1f_{7/2}$ and $1f_{5/2}$ proton orbitals. Because of the dominance of spin-transfer strength in the (p,n) reaction at medium energies, these transitions are strong and provide important tests of reaction-mechanism and nuclear-structure models.

In two earlier papers, Anderson *et al.*^{1,2} presented and discussed cross section measurements for the $^{48}\text{Ca}(p,n)^{48}\text{Sc}$ reaction at 134 and 160 MeV. These papers showed that the cross section angular distributions for the excitation of the $(f_{7/2}, f_{7/2}^{-1})$ particle-hole ($1p1h$) band and for the strongly excited 1^+ state spectrum can be described reasonably well by distorted-wave-impulse-approximation (DWIA) calculations which use "reasonable" $1f$ - $2p$ shell-model wave functions. We present here experimental analyzing-power measurements for these same transitions in the $^{48}\text{Ca}(p,n)^{48}\text{Sc}$ reaction. These measurements provide further tests of the assumed models and increased sensitivity to certain aspects of the theoretical descriptions. Excitation-energy plots are presented and discussed also. It is especially interesting to see whether such plots can provide a signature of spin-transfer strength for this

reaction in order to look for such strength in the continuum above the Gamow-Teller giant resonance (GTGR).

II. EXPERIMENTAL PROCEDURE

The experiment was performed at the Indiana University Cyclotron Facility (IUCF) with the beam-slinger system.³ Neutron energies were measured by the time-of-flight technique. The neutrons were detected in large-volume, mean-timed neutron detectors⁴ placed in three separate detector stations at angles of 0° , 24° , and 45° with respect to the undeflected proton beam. The flight paths to the two forward-angle stations were both 71.0 ± 0.2 m; that to the wide-angle station was 37.3 ± 0.2 m. The overall timing resolutions in the various detectors varied from about 0.60 to 0.75 ns. These timing resolutions included contributions from the beam burst width, the target thickness, the finite thicknesses of the neutron detectors, and the intrinsic timing resolutions of the detectors. These timing resolutions provided energy resolutions of about 400 keV in the first two detector stations and about 700 keV in the wide-angle station. The neutron detectors and the time-of-flight arrangement were similar to those described earlier.¹

The calcium target was enriched to 97.3% and contained 28.5 ± 0.5 mg/cm² of ^{48}Ca . Beam integration was performed by a well-shielded split Faraday cup located approximately 10 m downstream from the target. Neutron detector efficiencies were calculated with the Monte Carlo efficiency code of Cecil *et al.*⁵ Pulse-height calibrations were performed periodically for each neutron detector with standard γ -ray sources and a calibrated fast amplifier. In order to avoid problems associated with long-

term drifts in detector responses or beam fluctuations which might introduce false asymmetries, the beam polarization state was "flipped" every 60 s.

The analyzing power $A_y(\theta)$ for the (p,n) reaction is

$$A_y(\theta) = \frac{N_{\uparrow}(\theta) - N_{\downarrow}(\theta)}{P_{\uparrow}N_{\uparrow}(\theta) + P_{\downarrow}N_{\downarrow}(\theta)}, \quad (1)$$

where $N_{\uparrow}(\theta)$ and $N_{\downarrow}(\theta)$ are the yields in a single detector and P_{\uparrow} and P_{\downarrow} are the beam polarizations for the spin-up and spin-down states of the proton beam. For $P_{\uparrow} = P_{\downarrow} = P_b$, the analyzing power $A_y(\theta)$ is the asymmetry $\epsilon [= (N_{\uparrow} - N_{\downarrow}) / (N_{\uparrow} + N_{\downarrow})]$ divided by the beam polarization P_b . The polarized proton beam was provided by the IUCF atomic-beam polarized ion source. The beam polarization P_b was typically about 70% as determined with a ^4He polarimeter located between the injector and main cyclotrons.⁶

III. DATA REDUCTION

The data were recorded during the experimental runs event by event for each neutron detector. The neutron time of flight, the detector pulse height, and the spin state of the polarized beam was recorded for each event. The event tapes were later replayed at various pulse-height thresholds in order to extract time-of-flight spectra, excitation-energy spectra, cross sections, and analyzing powers. The pulse-height thresholds were varied in order to reduce background (primarily from overlap of slow neutrons from the preceding beam burst) while maintaining reasonable detector efficiency (which decreases with increasing threshold values).

Excitation-energy spectra were obtained from the measured time-of-flight spectra by using the known flight path and the calibration of the time-to-amplitude converter. Known excitation energies of states in ^{48}Sc were taken in a manner similar to that discussed in Refs. 1 and 2. Simple peak summing and/or Gaussian peak fitting were used to extract the yields of individual transitions for both spin-down and spin-up spectra. Examples of the peak fitting for this reaction were presented in Ref. 1. Excitation-energy spectra of analyzing powers for this reaction were extracted from the time-of-flight spectra measured for each spin state and binned appropriately.

The uncertainties presented for the analyzing-power results include the statistical and fitting uncertainties in the extracted neutron sums for spin up and spin down, combined with an estimated uncertainty of $\pm 5\%$ in the beam polarization. The fitting uncertainty is obtained from the error matrix of the fitting program⁷ and reflects an additional uncertainty associated with the quality of the fit. The measured analyzing powers could be tested at 0° , where the analyzing power is known to be zero. As seen in Figs. 1–7, four of the six 0° measurements are indeed zero, within the estimated uncertainties. This result is consistent with that expected if the errors are statistical only and there are no sources of false asymmetries present in either the measurements or the data reduction. The combined result for the six cases is -0.006 ± 0.009 , taken as the weighted average of all six results. This result is

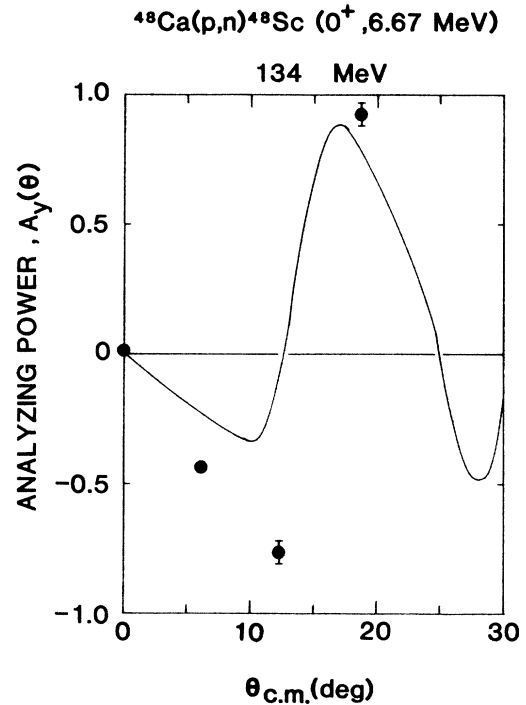


FIG. 1. Analyzing-power angular distribution for the $^{48}\text{Ca}(p,n)^{48}\text{Sc}$ reaction at 134 MeV to the 0^+ (IAS) state at 6.67 MeV. Shown also are DWIA calculations as discussed in the text.

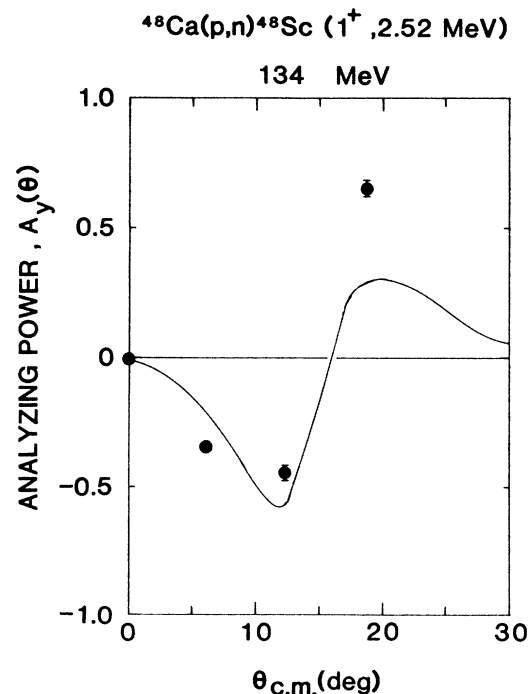


FIG. 2. Analyzing-power angular distribution for the $^{48}\text{Ca}(p,n)^{48}\text{Sc}$ reaction at 134 MeV to the 1^+ state at 2.52 MeV. Shown also are DWIA calculations as discussed in the text.

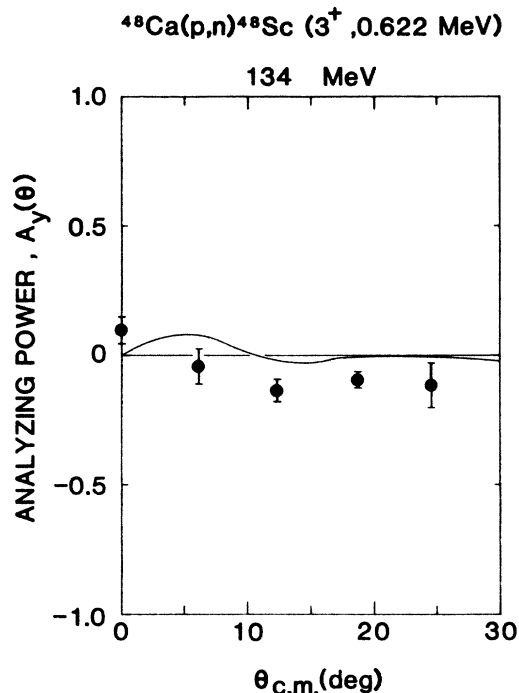


FIG. 3. Analyzing-power angular distribution for the $^{48}\text{Ca}(p,n)^{48}\text{Sc}$ reaction at 134 MeV to the 3^+ state at 0.62 MeV. Shown also are DWIA calculations as discussed in the text.

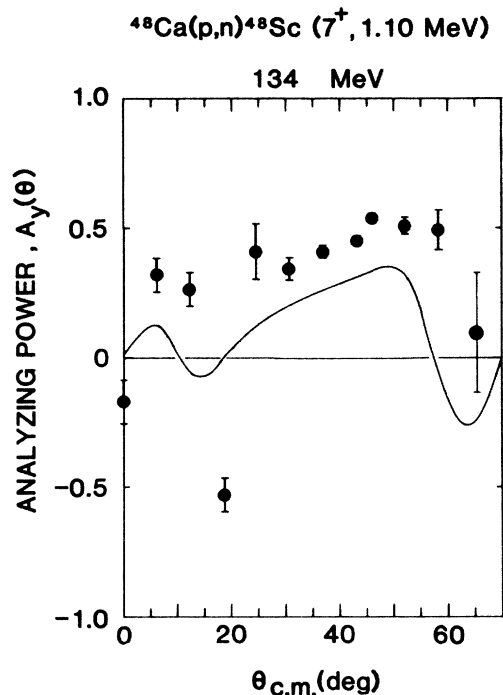


FIG. 5. Analyzing-power angular distribution for the $^{48}\text{Ca}(p,n)^{48}\text{Sc}$ reaction at 134 MeV to the $2^+, 7^+$ complex at 1.1 MeV. Shown also are DWIA calculations as discussed in the text.

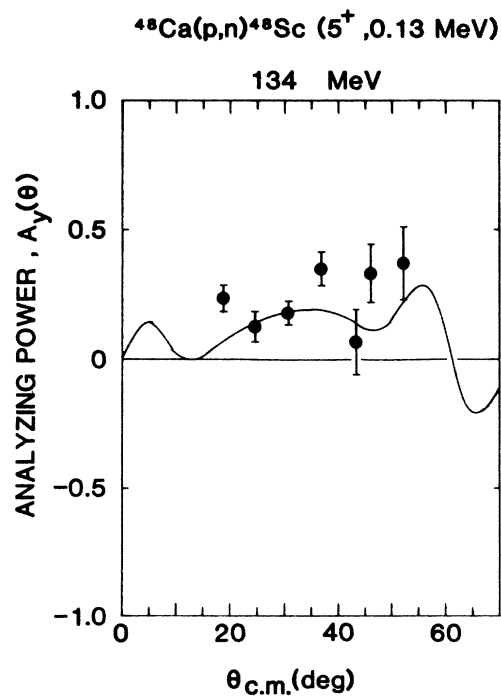


FIG. 4. Analyzing-power angular distribution for the $^{48}\text{Ca}(p,n)^{48}\text{Sc}$ reaction at 134 MeV to the $4^+, 5^+, 6^+$ complex between 0 and 0.2 MeV. Shown also are DWIA calculations as discussed in the text.

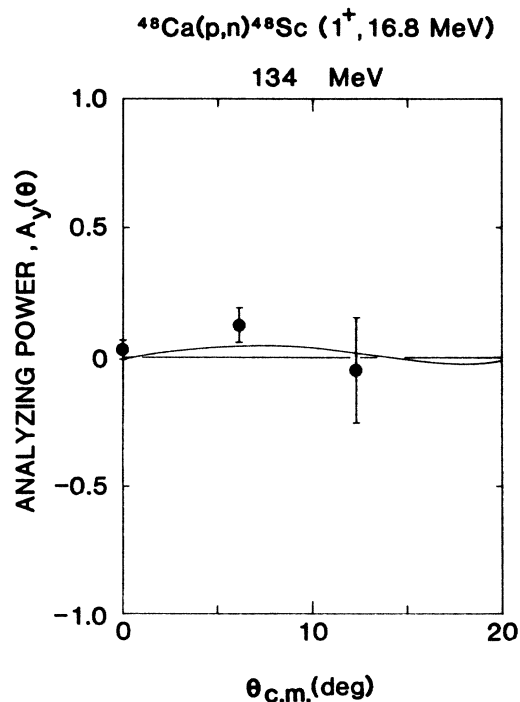


FIG. 6. Analyzing-power angular distribution for the $^{48}\text{Ca}(p,n)^{48}\text{Sc}$ reaction at 134 MeV to the 1^+ state at 16.8 MeV. Shown also are DWIA calculations as discussed in the text.

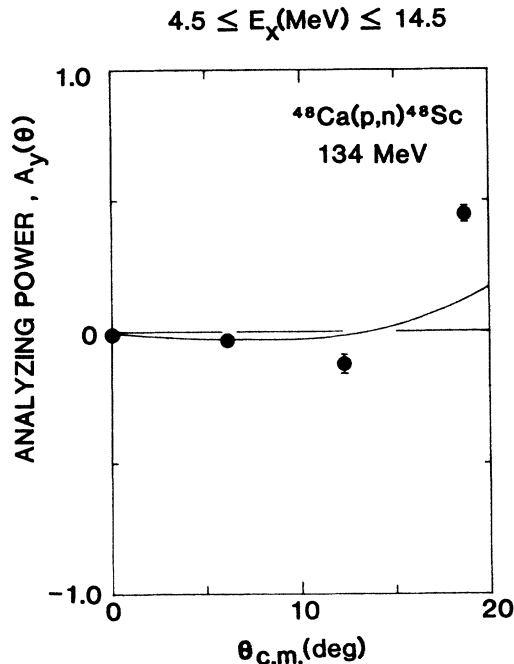


FIG. 7. Analyzing-power angular distribution for the $^{48}\text{Ca}(p,n)^{48}\text{Sc}$ reaction at 134 MeV to the 1^+ Gamow-Teller giant resonance (GTGR) between 4.5 and 14.5 MeV of excitation. Shown also are DWIA calculations as discussed in the text.

supported also by the excitation-energy plot of 0.3° shown in Fig. 8. The statistical fluctuations in A_y go both above and below, but narrow down to almost exactly zero in the region of the GTGR, where the statistics are best.

IV. RESULTS AND DISCUSSION

The data were analyzed to obtain analyzing powers both for strong individual transitions and for excitation-energy spectra. The results for individual transitions are presented first, compared with distorted-wave-impulse-approximation calculations. The results for excitation-energy plots are presented last and are useful for considering strength observed in the nuclear continuum.

A. Individual transitions

Analyzing-power angular distributions were extracted for the transitions to the 0^+ isobaric analog state (IAS) at 6.67 MeV, the 1^+ state at 2.52 MeV, the 3^+ state at 0.62 MeV, the $4^+, 5^+, 6^+$ complex between 0 and 0.2 MeV, and the $2^+, 7^+$ complex at 1.1 MeV. These transitions are to the well-known⁸ members of the $(f_{7/2}, f_{7/2}^-)$ octet of $1p1h$ states in ^{48}Sc . Analyzing-power angular distributions were extracted also to the 1^+ ($T=4$) state at 16.8 MeV and to the 1^+ Gamow-Teller giant resonance complex between 4.5 and 14.5 MeV. The experimental results are shown in Figs. 1–7. The experimental angular distributions are compared with DWIA calculations for these transitions. The calculations are entirely similar to those presented in Refs. 1 and 2 for comparison with cross-section angular distributions. They were performed with

the code DWBA70 (Ref. 9) with the N-N effective interaction of Love and Franey,¹⁰ optical-model parameters from the global parameters of Schwandt *et al.*,⁶ and shell-model wave functions which include some $2p2h$ ground-state correlations in the $1f-2p$ shell.¹

The experimental angular distributions for the 0^+ (6.67 MeV) and 1^+ (2.52 MeV) transitions are similar and the DWIA calculations predict the general shape, although precise agreement is certainly not seen. The angular distribution for the 3^+ (0.62 MeV) transition is relatively flat and again is described reasonably well by the DWIA calculations. The angular distribution presented in Fig. 4 is to the $4^+, 5^+, 6^+$ complex between 0 and 0.20 MeV; however, as discussed in Ref. 1, the 5^+ state dominates this complex and we show in Fig. 4 the DWIA prediction for the analyzing power for this state alone. Especially considering the statistical errors of the data, good agreement is generally observed. The angular distribution presented in Fig. 5 is to the $2^+, 7^+$ complex at 1.1 MeV. As shown in Ref. 1, the 2^+ strength dominates only at very forward angles and the 7^+ , “ $0h\omega$ ” stretched-state strength dominates at angles larger than about 25° . We show here only the DWIA prediction for the 7^+ transition, but we note that the 2^+ prediction agrees reasonably well in shape out to about 15° . The DWIA prediction for the analyzing powers from the 7^+ transition is seen to have the correct general shape at wide angles, but to be somewhat too small in absolute magnitude. We observed similar agreement between standard DWIA calculations and experimental analyzing powers for the “ $1h\omega$ ” stretched-state excitations in the $^{16}\text{O}(p,n)^{16}\text{F}(4^-)$ and $^{28}\text{Si}(p,n)^{28}\text{P}(6^-)$ reactions at 135 MeV.^{11,12} This shape, with positive analyzing powers out to near 60° and then a relatively rapid swing toward negative analyzing powers, appears to be characteristic of isovector stretched-state transitions.

In Fig. 6 we show the experimental angular distribution for analyzing powers for the transition to the $T=4$, 1^+ state at 16.8 MeV. This state is the analog of the known 1^+ , $M1$ state in ^{48}Ca ,¹³ and is part of the so-called Gamow-Teller strength in the (p,n) reaction. The experimental analyzing powers are seen to go slightly positive away from 0° , and to be reproduced well by the DWIA prediction. Finally, in Fig. 7 we show the angular distribution of the analyzing power for the large GTGR observed between 4.5 and 14.5 MeV of excitation. The backgrounds assumed in the spin-down and spin-up spectra for the GTGR were simple straight-line backgrounds from just below to just above the GTGR. These backgrounds are sometimes referred to as “experimentalist’s backgrounds.” While such backgrounds probably subtract some GT strength, they have the advantages of being well defined and consistent for both spin states; furthermore, we find that the analyzing powers at forward angles (out to 12°) are changed only slightly if no background at all is subtracted. (See Refs. 2 and 14 for a further discussion of the background under the GTGR.) As shown in Ref. 1, this resonance actually consists of many individual but overlapping states with a distribution in good agreement with the 1^+ spectrum predicted using the $1f-2p$ wave functions of Brown (described in Refs. 1 and 2). The DWIA calculation shown in Fig. 7 is the cross-section

weighted average of the eighteen 1^+ states predicted to make up this resonance. The agreement between the calculation and the data is seen to be good, except at the widest angle.

The most significant observation in these several comparisons is the generally good agreement of the “standard” DWIA calculations with the experimental shapes. Note that the various analyzing-power angular distributions sometimes show qualitatively different shapes—and that the DWIA calculations correctly predict these general shapes. Precise agreement between the calculations and the experimental results is certainly not always observed; however, the ability of the calculations to predict correctly the general shapes of the different transitions is striking. Note that these various transitions include low-spin through high-spin states, so that the calculations are tested from low-momentum to high-momentum transfers. This general agreement between standard DWIA calculations and experimental angular distributions is well known for the (p,p') reaction at this incident energy;¹⁵ however, the data presented here represent the first such comparisons for the (p,n) reaction, except for the two stretched-state transitions mentioned above,^{11,12} which also show good general agreement. We find that the DWIA calculations are sensitive to the inclusion of all of the major ingredients [i.e., distorted waves, all of the major terms in the N-N effective interaction (including the spin-orbit term), and reasonable nuclear-structure wave functions]. We find that the DWIA calculations are not very sensitive, at least for the general shape of the angular distributions, to small reasonable changes in the various parameters involved. The conclusion indicated by the generally good agreement seen here, for a reaction which should be a good test case, is that the standard DWIA is a good first-order theory for the (p,n) reaction at this energy.

It is significant that the measured and predicted analyzing-power angular distributions to both the low-lying 1^+ state at 2.52 MeV and to the 0^+ (IAS) at 6.67 MeV are similar. Both of these final states have predominant $(f_{7/2}, f_{7/2}^{-1})$ 1p1h structures.¹ The transition to the 1^+ state necessarily involves spin transfer and is part of the Gamow-Teller strength in this reaction.² The transition to the 0^+ (IAS) does not involve spin transfer and corresponds to the “Fermi” strength in this reaction. Thus we see clearly that the analyzing power is not a useful observable for identifying spin-transfer strength in the (p,n) reaction, at least in this case.

Next, we note that the angular distribution to the high-lying 1^+ state at 16.8 MeV differs qualitatively from that to the low-lying 1^+ state at 2.52 MeV; in particular, the analyzing powers go slightly positive away from 0° for the 16.8 MeV state transition compared to going strongly negative for the 2.52 MeV state transition. The DWIA calculations, without adjustment from those presented in Refs. 1 and 2, correctly predict this behavior. The explanation for this qualitative change is not due simply to the different Q values involved; DWIA calculations for the two states retain their characteristic shapes when the Q values are “switched.”

The explanation for this change in shape of the

analyzing-power angular distribution is due almost certainly to the change in the structure of the two final (1^+) states. All three transitions are dominated by the central term of the N-N effective interaction and both of the 1^+ transitions involve spin transfer. The most obvious difference is that the low-lying states are believed to be predominantly $(f_{7/2}, f_{7/2}^{-1})$, while the high-lying, $T=4$, 1^+ state is believed to be predominantly $(f_{5/2}, f_{7/2}^{-1})$.² Thus, the difference appears to be related to whether the particle-hole excitation involves only the same orbital or proceeds to the spin-orbit partner.

The qualitative effect seen here for these transitions is likely related to the so-called $P-A$ topic. This subject was discussed recently by Love and Comfort,¹⁶ who find that current \otimes spin couplings are important for understanding P and A differences in unnatural-parity transitions in (p,n) reactions, such as the 0^+ to 1^+ transitions considered here. The importance of P and A differences for analyzing power measurements alone can be seen by writing the analyzing power as

$$A = \frac{P+A}{2} - \frac{P-A}{2}, \quad (2)$$

and considering the two terms separately. For a 0^+ to 1^+ transition in the $^{90}\text{Zr}(p,p')$ reaction at 200 MeV, Love and Comfort find that the first term is sensitive to the spin-orbit term in both the optical model and the N-N interactions, while the second term is not; however, they find also that the second term is quite sensitive to the orbital involved while the first term is not. They note that this sensitivity involved for the $P-A$ term arises in their calculations from a nonlocality (or velocity dependence) in the spin-dependent part of the N-N interaction. Love and Comfort show that for transitions within a single shell, one of the nonvanishing form factors required for $P=A$ is specified by the matrix element of the operator $\langle i\mathbf{L} \times \boldsymbol{\sigma} \rangle$. In terms of the $\langle \boldsymbol{\sigma} \rangle$ operator, they show that this matrix element is

$$\langle j' || i\mathbf{L} \times \boldsymbol{\sigma} || j \rangle = (j-j')j_{>} \langle j' || \boldsymbol{\sigma} || j \rangle, \quad (3)$$

where j and j' are the initial and final j values of the single particle orbitals and $j_{>}$ is the greater of j and j' . From this expression, we see that this particular matrix element will vanish for $j'=j$, so that we would not expect a contribution to the low-lying 1^+ state with the predominant 1p1h configuration $(f_{7/2}, f_{7/2}^{-1})$. The qualitative effect we see in the experimental data, together with the good agreement of the theoretical calculations, suggests that such contributions are significant and are treated reasonably well in the calculations.

B. Excitation-energy plots of the analyzing power

In addition to the analyzing-power angular distributions for individual transitions, we extracted excitation-energy plots of the analyzing power at each angle. Such plots, up to $E_x=40$ MeV, are shown in Figs. 8 and 9. It is useful to look at such plots for possible characteristic analyzing-power signatures of giant resonances, such as the GTGR or the $L=1$ giant resonance, and also to study excitation of the nuclear continuum.

At 0° , we see that the analyzing power is consistent statistically with zero over the entire excitation-energy range, as expected. At 6° and 12° one sees the relatively large negative analyzing powers of the low-lying 1^+ and 0^+ (IAS) states, discussed above. The GTGR, which begins just above the 1^+ state, is seen to have negative analyzing power at low excitation energies; but as the excitation energy increases, the analyzing powers shift gradually to positive values. This result is consistent with our earlier conclusion² that the individual states comprising the GTGR shift from predominantly $(f_{7/2}, f_{7/2}^{-1})$ at low excitation energies to predominantly $(f_{5/2}, f_{7/2}^{-1})$ at higher excitation energies. Thus the shift in the analyzing power with increasing excitation energy is probably just a reflection of the different characteristic analyzing powers of these two 1p1h structures, as discussed above. This conclusion must be qualified somewhat since the $\Delta L = 1$ giant resonance also contributes in this region.

At wider angles, one sees the effects of the various members of the $(f_{7/2}, f_{7/2}^{-1})$ 1p1h band at low excitation energies, as they come and go, until at about 36° one sees the low excitation-energy region dominated by the characteristic positive analyzing power of the 7^+ , " $0\hbar\omega$ " stretched state.

The continuum region, from 20 up to 40 MeV (which is the maximum excitation energy available in these measurements), has an analyzing power close to zero at all angles. The 6° spectrum exhibits a small positive analyzing power up to about 30 MeV, which is probably due to the

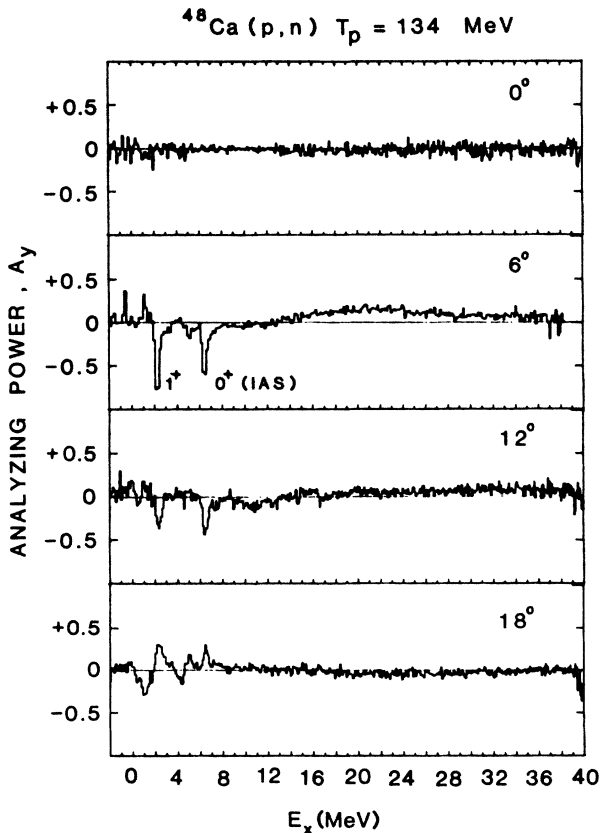


FIG. 8. Analyzing-power excitation-energy spectra for the $^{48}\text{Ca}(p,n)^{48}\text{Sc}$ reaction at 134 MeV at angles from 0° to 18° .

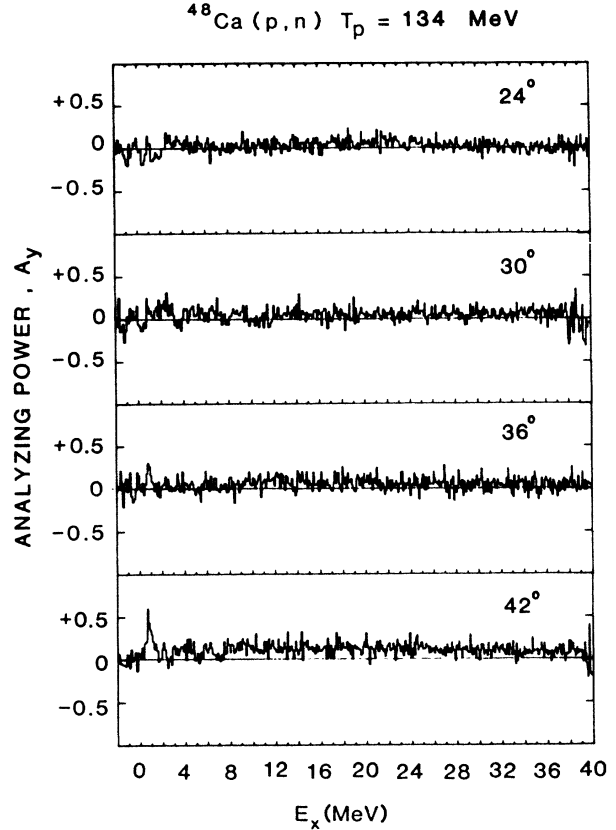


FIG. 9. Analyzing-power excitation-energy spectra for the $^{48}\text{Ca}(p,n)^{48}\text{Sc}$ reaction at 134 MeV at angles from 24° to 45° .

$L = 1$ giant resonance, which occurs in this region, as can be seen in the cross section excitation energy plots of Ref. 1. A careful study of the excitation of this giant resonance requires an analysis of the underlying continuum background and will not be attempted here. The widest-angle spectrum exhibits a consistent small positive analyzing power in the continuum, but the statistics are marginal.

V. CONCLUSIONS

The analyzing-power measurements for the $(f_{7/2}, f_{7/2}^{-1})$ particle-hole band of states excited in the $^{48}\text{Ca}(p,n)^{48}\text{Sc}$ reaction agree reasonably well with simple DWIA calculations. Qualitatively, different shapes are observed for the analyzing-power angular distributions for most of these transitions, and these different shapes are indicated by the DWIA calculations. We note that the analyzing-power calculations are sensitive to the various ingredients of the DWIA, viz., the assumed one-step mechanism, the distorted waves, and the relative strengths of the various terms in the N-N effective interaction. The fact that the agreement is good for several transitions indicates that these ingredients are probably reasonable, and that these states are predominantly 1p1h in their structures. We note that the DWIA calculations are quite conventional.

They use a standard DWIA reaction-mechanism code, global optical-model parameters without “wine-bottle” shapes, and a popular N-N effective interaction without density dependence. Earlier measurements^{17,15} led to the conclusion that the (p,n) and (p,p') reactions are predominantly single-step reactions above about 100 MeV. These results support that conclusion; furthermore, as noted by Kelly and Carr,¹⁸ and shown by Love *et al.*,¹⁹ isovector spin-transfer transitions are much less sensitive to density-dependent effects than isoscalar transitions. Finally, the need for wine-bottle shapes in the optical-model potential wells is indicated more clearly at higher energies (viz., 200–500 MeV).²⁰ Thus, at this energy, it may be that the good description by the simple DWIA for this reaction is somewhat fortuitous; however, because both cross sections and analyzing powers are described well, the (p,n) reaction at this energy appears to provide a good tool for extracting spectroscopic information.

The transitions to the low-lying 1^+ state at 2.52 MeV and 0^+ state at 6.67 MeV exhibit similar shapes for their analyzing-power angular distributions. This shape differs qualitatively from that observed for the transition to the 1^+ state at 16.8 MeV. The low-lying 1^+ and 0^+ transi-

tions are predominantly spin-transfer and non-spin-transfer, respectively; however, they both have predominant ($f_{7/2}, f_{7/2}^{-1}$) structure, whereas the 16.8 MeV, 1^+ state is predominantly ($f_{5/2}, f_{7/2}^{-1}$). Thus, for these transitions the shapes of the analyzing-power angular distributions appear to be influenced more by the nuclear structure than by whether the transition involves spin transfer or not. This difference may be due to a sensitivity of the analyzing power to nonlocality (or velocity-dependent) effects which are different for the two $1p1h$ configurations.

ACKNOWLEDGMENTS

We are grateful to the staff of the Indiana University Cyclotron Facility for their assistance during the running of this experiment. We profited from detailed discussions with Peter Tandy and Robert McCarthy regarding the reaction mechanisms involved, with Alex Brown regarding the structure calculations, and with Gary Love regarding the relationship of the present experiment to the $P-A$ topic. This work was supported in part by the National Science Foundation under Grant Nos. PHY 82-00562, PHY 85-01054, and PHY 81-14339.

*Present address: Los Alamos National Laboratory, Los Alamos, NM 87545.

¹B. D. Anderson, T. Chittrakarn, A. R. Baldwin, C. Lebo, R. Madey, R. J. McCarthy, J. W. Watson, B. A. Brown, and C. C. Foster, *Phys. Rev. C* **31**, 1147 (1985).

²B. D. Anderson, T. Chittrakarn, A. R. Baldwin, C. Lebo, R. Madey, P. C. Tandy, J. W. Watson, B. A. Brown, and C. C. Foster, *Phys. Rev. C* **31**, 1161 (1985).

³C. D. Goodman, C. C. Foster, M. B. Greenfield, C. A. Goulding, D. A. Lind, and J. Rapaport, *IEEE Trans. Nucl. Sci.* **NS-26**, 2248 (1979).

⁴R. Madey, J. W. Watson, M. Ahmad, B. D. Anderson, A. R. Baldwin, A. L. Casson, W. Casson, R. A. Cecil, A. Fazely, J. N. Knudson, C. Lebo, W. Pairsuwan, P. J. Pella, J. C. Varga, and T. R. Witten, *Nucl. Instrum. Methods* **214**, 401 (1983).

⁵R. Cecil, B. D. Anderson, and R. Madey, *Nucl. Instrum. Methods* **161**, 439 (1979).

⁶P. Schwandt, H. O. Meyer, W. W. Jacobs, A. D. Bacher, S. E. Vigdor, M. D. Kaitchuck, and T. R. Donoghue, *Phys. Rev. C* **26**, 55 (1982).

⁷P. R. Bevington, K. G. Kibler, and B. D. Anderson, Case Western Reserve University No. C00-1573-63, 1969 (unpublished); P. R. Bevington, *Data Reduction and Error Analysis for the Physical Sciences* (McGraw-Hill, New York, 1969), p. 237.

⁸H. Ohnuma, J. R. Erskine, J. P. Schiffer, J. A. Nolen, and N. Williams, *Phys. Rev. C* **1**, 496 (1970); H. Ohnuma and J. L. Yutema, *ibid.* **2**, 1725 (1970).

⁹J. Raynal and R. Schaeffer, computer code DWBA70. The version we used was supplied to us by W. G. Love.

¹⁰W. G. Love and M. A. Franey, *Phys. Rev. C* **24**, 1073 (1981).

¹¹R. Madey, A. Fazely, B. D. Anderson, A. R. Baldwin, A. M. Kalenda, R. J. McCarthy, P. C. Tandy, J. W. Watson, W. Bertozzi, T. Buti, M. Finn, M. Kovash, B. Pugh, and C. C. Foster, *Phys. Rev. C* **25**, 1715 (1982).

¹²A. Fazely, R. Madey, B. D. Anderson, A. R. Baldwin, C. Lebo, P. C. Tandy, J. W. Watson, W. Bertozzi, T. Buti, M. Finn, C. Hyde-Wright, J. Kelly, M. A. Kovash, B. Murdock, B. Pugh, and C. C. Foster, *Nucl. Phys.* **A443**, 29 (1985).

¹³G. M. Crawley, N. Anantaraman, A. Galonsky, C. Djalali, N. Marty, M. Morlet, A. Willis, and J.-C. Jourdain, *Phys. Lett.* **127B**, 322 (1983).

¹⁴J. W. Watson, B. D. Anderson, A. R. Baldwin, T. Chittrakarn, B. S. Flanders, and R. Madey, in *Antinucleon- and Nucleon-Nucleus Interactions*, edited by G. E. Walker *et al.* (Plenum, New York, 1985), p. 373.

¹⁵A. D. Bacher, in *Polarization Phenomena in Nuclear Physics—1980*, AIP Conf. Proc. No. 69, edited by G. G. Ohlsen *et al.* (AIP, New York, 1981), p. 220.

¹⁶W. G. Love and J. R. Comfort, *Phys. Rev. C* **29**, 2135 (1984).

¹⁷B. D. Anderson, A. Fazely, C. Lebo, J. W. Watson, and R. Madey, *Spin Excitations in Nuclei*, edited by F. Petrovich *et al.* (Plenum, New York, 1984), p. 391.

¹⁸J. Kelly and J. A. Carr, in *Spin Excitations in Nuclei*, Ref. 17, p. 253.

¹⁹W. G. Love, A. Klein, and M. A. Franey, in *Antinucleon- and Nucleon-Nucleus Interactions*, Ref. 14, p. 1.

²⁰H. O. Meyer, P. Schwandt, W. W. Jacobs, and J. R. Hall, *Phys. Rev. C* **27**, 459 (1983).